# Effect of MAX Phase Mo<sub>2</sub>TiAlC<sub>2</sub> on the PVDF Ultrafiltration Membrane Properties and Performance

H.M.S.N. Bandara and W.J.M. Samaranayaka\*

Department of Physics and Electronics, University of Kelaniya, Kelaniya, Sri Lanka

**Abstract:** Ultrafiltration membranes are widely used in wastewater filtration due to their efficiency relative to conventional water treatment technologies. To improve the antifouling property of the PVDF membrane, a composite ultrafiltration membrane was fabricated employing the *in-situ* embedment approach throughout the phase inversion process and utilizing a new 2D material, MAX phase Molybdenum Titanium Aluminium Carbide (Mo<sub>2</sub>TiAlC<sub>2</sub>). The membranes were described using Fourier transform infrared spectroscopy (FTIR), Scanning electron microscopy (SEM), and porosity measurements. Rejection tests were applied to study the produced membranes. Adding Mo<sub>2</sub>TiAlC<sub>2</sub> increased the hydrophilicity of the composite membrane compared to the pristine membrane. Porosity and membrane pore size increased with the addition up to 0.6% wt. The most hydrophilic membrane (M3) recorded the highest protein rejection of 84.9%, which was much higher than that of the pristine membrane. These findings highlight the potential of Mo<sub>2</sub>TiAlC<sub>2</sub> as a promising PVDF membrane additive.

**Keywords:** Hydrophilicity, MAX phase Mo<sub>2</sub>TiAlC<sub>2</sub>, ultrafiltration, PVDF, membrane.

# 1. INTRODUCTION

Ultrafiltration (UF) is a low-pressure membrane process widely applied in water treatment due to its high separation efficiency and compact design [1]. UF membranes, which are available in both polymeric and ceramic forms, effectively remove various pollutants and microorganisms from water [2]. The technology has found applications across diverse industries, including textiles, dairy, and pharmaceuticals [2]. Recent advancements have focused development of tight UF membranes with smaller pore sizes (300-5000 Da) to improve the rejection of trace organic compounds and reduce fouling [3]. However, challenges such as low water flux and high operating pressure still need to be addressed [3]. UF membranes have become increasingly important in drinking water production as a safety barrier against bacteria and viruses, and in wastewater treatment for solute separation and water reuse [4]. The growing demand for improved membranes is driven by the increasing prevalence of water pollution and the associated treatment challenges.

Polyvinylidene fluoride (PVDF) is one of the most widely used materials for ultrafiltration membranes owing to its excellent properties. PVDF exhibits high mechanical strength, good thermal and chemical stability, resistance to aging, and favorable film-forming ability [5, 6]. These characteristics make PVDF

membranes suitable for various water treatment applications. However, the hydrophobic nature of PVDF leads to membrane fouling issues, which is a significant limitation [7, 8]. To address this challenge, researchers have developed various modification strategies to enhance the hydrophilicity and antifouling performance of PVDF membranes. These include surface coating, blending with hydrophilic materials, and chemical modifications such as amination and grafting [7, 8]. These modifications aim to improve membrane wettability, reduce organic fouling, and enhance overall filtration efficiency while maintaining PVDF's desirable properties [6, 8].

Membrane modification techniques can be broadly categorised into surface modification, physical blending (or doping), and chemical grafting [9]. Surface modification techniques involve hydrophilization, heating, and coating [9]. Chemical grafting can be achieved through "rafting-to" or "grafting-from" techniques [9]. Physical blending involves incorporating additives into the membrane matrix during synthesis [10]. Nanomaterial incorporation is a widely used and effective method due to its simplicity, cost-effectiveness, and minimal structural disruption [9]. Various nanomaterials, such as metal nanoparticles, zeolites, and carbon nanotubes, have been successfully integrated into membranes [9]. Other modification techniques include plasma treatment, surfactant modification, and polymer blending [10]. These modifications aim to improve membrane hydrophilicity, reduce fouling, and enhance overall performance [11, 12]. Emerging materials like polydopamine offer promising opportunities for membrane surface modification [12].

E-ISSN: 1929-5995/25

<sup>\*</sup>Address correspondence to this author at the Department of Physics and Electronics, University of Kelaniya, Kelaniya, Sri Lanka; E-mail: janaki@kln.ac.lk

MAX phases are layered ternary carbides/nitrides with a general formula  $M_{n+1}AX_n$ , where M is a transition metal, A is an A-group element, and X is carbon or nitrogen [13]. Their structure consists of  $M_{n+1}AX_n$ sheets interleaved with A layers, resulting in a combination of metallic and ceramic properties [14]. MXenes, which are two-dimensional derivatives of MAX phases, are obtained by selectively etching the A layer through chemical treatment [13]. Mo<sub>2</sub>TiAlC<sub>2</sub> is a specific MAX phase compound that can be transformed into Mo<sub>2</sub>TiAlC<sub>2</sub> MXene [15]. MXenes exhibit high hydrophilicity and electrical conductivity [13]. Mo<sub>2</sub>TiAlC<sub>2</sub> demonstrates mechanical stability and metallic electrical conductivity, with Mo 4d states dominating at the Fermi level [16]. The derived Mo<sub>2</sub>TiAlC<sub>2</sub> MXene shows improved catalytic activity for hydrogen evolution reaction over time, attributed to MoO<sub>2</sub> formation [15].

Recent studies have demonstrated the effectiveness of incorporating nanofillers like graphene oxide (GO) and MXene into PVDF membranes to enhance their performance. These modifications have led to increased water permeability, with flux improvements ranging from 48% to 240% compared to pristine PVDF membranes [17-19]. The addition of nanofillers also significantly improved membrane hydrophilicity, as evidenced by reduced water contact angles [17, 20]. Furthermore, the modified membranes exhibited enhanced antifouling properties and dye rejection capabilities. For instance, GO-ZnO/PVDF membranes showed a substantial reduction in irreversible fouling ratio for bovine serum albumin [18], while MXene-modified GO/PVDF membranes demonstrated 100% removal of crystal violet dye [20]. These improvements in membrane performance were attributed to the synergistic effects of the nanofillers, including their high specific surface area and oxygen-containing functional groups [17].

# 2. MATERIALS AND METHODS

## 2.1. Materials

Polyvinylidene fluoride (PVDF) (Mw =  $\sim$  534,000, Sigma-Aldrich, product no. 427152), polyvinylpyr-

rolidone (PVP) (Mw =  $\sim$  40,000, Sigma-Aldrich, product no. PVP40), N-methyl-2-pyrrolidone (NMP) (Carl Roth, product no. 4306.1,  $\geq$  99%), and Mo<sub>2</sub>TiAlC<sub>2</sub> MAX Phase powder (200mesh, 99%) was obtained by BEIJING 33ENE TECHNOLOGY CO., LTD, China. All chemicals were of analytical grade and used without further purification.

# 2.2. Membrane Preparation

The first preparation was made at room temperature, with stirring for 2 hours to homogeneously distribute the Mo<sub>2</sub>TiAlC<sub>2</sub> MAX Phase nanoparticles in the solvent. After that, the stirring rates were gradually increased from 800 rpm to about 1600 rpm to enable proper dispersion of the nanoparticles. After dispersion, the vessel containing the mixture was then put into a water bath at about 60°C. This controlled heating ensured the gradual dissolution of the PVDF pellets and PVP powder into the stirring NMP solution. While the polymers were dissolving, the viscosity of the solution gradually increased, naturally reducing the stirring speed. Careful handling resulted in a homogeneous and well-dispersed resultant mixture ready for membrane casting. This was then poured on the borosilicate plate and compressed with another plate to yield the membrane. The thickness of the membrane was controlled by the Scotch tape method, where a number of superimposed layers of Scotch tape provide a particular thickness. This was to ensure that the compressed solution was completely soaked in distilled water for two days for the complete solidification of the membrane and to ensure that there were no residual solvents and impurities left behind. The Scotch tape method was employed as an alternative phase inversion technique due to the unavailability of a Doctor Blade, while still ensuring precise control over the membrane thickness. Further, post-treatment was carried out by dipping the membrane for two days in isopropanol and then for two days in glycerol to enhance its stability and keep it from becoming brittle. The treated membrane was air-dried and stored for filtration applications.

Table 1: Composition of Samples with Varying MAX Phase Mo<sub>2</sub>TiAlC<sub>2</sub> Content

Sample Code	PVDF (%wt)	PVP (%wt)	NMP (%wt)	MAX Phase Mo <sub>2</sub> TiAlC <sub>2</sub> (%wt)
M1	20	2	78.0	0.0
M2	20	2	77.6	0.4
M3	20	2	77.4	0.6
M4	20	2	77.2	0.8

<sup>\*</sup>Composition percentages are by weight.

The MAX Phase concentration was optimized within the range of 0.1 wt% to 0.9 wt%, based on findings from previous research [21, 22].

## 2.3. Membrane Characterization

The morphology and the cross-section of the membranes were studied using a ZEISS EVO 15 Scanning Electron Microscope (SEM). Functional groups and chemical interactions of the membranes before and after incorporating Mo<sub>2</sub>TiAlC<sub>2</sub> MAX Phase and filtration were analyzed by Fourier transform infrared (FTIR) spectroscopy. Fourier transform infrared (FTIR) spectroscopy PerkinElmer Spectrum Two Fourier-transform infrared spectrometer (FTIR) was used to confirm the successful incorporation of Mo<sub>2</sub>TiAlC<sub>2</sub> MAX Phase and to analyze any chemical interactions between the membrane components. The membrane porosity was measured using the equation 1 [21],

$$\varepsilon\% = \frac{W_w - W_d}{A \times L \times \rho} \tag{1}$$

The W<sub>w</sub> was determined by immersing a piece of membrane in distilled water for 24 h, removing the

excess water using blotting paper, and measuring its weight [21]. The  $W_{\text{d}}$  was measured by oven drying the same membrane samples for 12 h and measuring their weights [21].

## where:

 $W_d$  = the membrane's dry weight (g)

 $W_{yy}$  = the membrane's wet weight (g)

 $A = \text{membrane area (cm}^2)$ 

 $\rho$  = water density = 1 g/cm<sup>3</sup>

L = thickness of the membrane (cm)

# 3. RESULTS AND DISCUSSION

# 3.1. Characterization of PVDF/ MAX Phase Mo<sub>2</sub>TiAIC<sub>2</sub> Membrane

# 3.1.1. Membrane Morphology and Porosity

The surface morphologies of the membranes (M1, M2, M3, and M4) were analyzed using SEM and the average pore distances were measured with ImageJ software. The Figure **1a**, **1b**, **1c**, and **1d** exhibit the

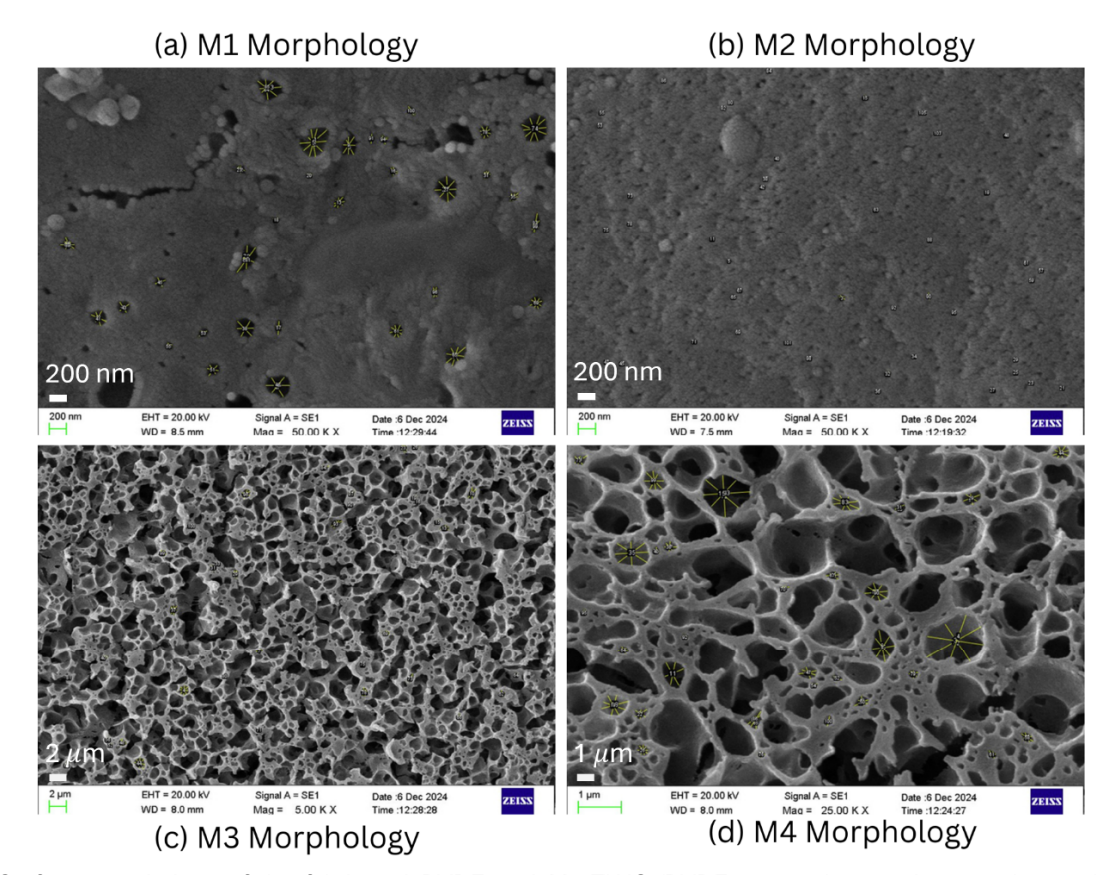


**Figure 1:** Surface morphology of the fabricated PVDF and Mo<sub>2</sub>TiAlC<sub>2</sub>/PVDF composite membranes observed under SEM, showing the effect of MAX phase incorporation on membrane structure.

surface morphology. The mean pore size values of M2, M3, and M4 are, respectively, 30nm, 650nm, and 1144nm.

The M1 membrane, which was unmodified, had unevenly distributed pores and cracks that tended to appear. In some places, aggregations were also seen. With the addition of  $Mo_2TiAlC_2$  MAX Phase, we can clearly see a pore formation that is evenly distributed than M1. The pore sizes are small, which is in the nano range. The M3 membrane has an increment in the pore size than the M2 membrane, and M4 has the largest pore size. All 4 membranes' thickness is kept in the 30  $\mu$ m to 50  $\mu$ m range. These results indicate that pore formation and pore size increase with the incorporation of  $Mo_2TiAlC_2$  MAX Phase, consistent with observations reported for other MAX Phase-based ultrafiltration membranes [21, 22].

The porosity has an optimum condition even though the pore size has increased, as shown in Figure 2. The highest porosity can be seen in the M3 membrane. While the lowest can be seen in the M2 membrane. The porosity and pore size were not assessed in the M1 membrane due to the aggregations and cracks in the membrane. From Figure 2 it is clear that with the increment of  $Mo_2TiAlC_2$  MAX Phase, the Pore Size increases, but not the porosity. By this result, we can clearly identify that, even though the size of a single pore increases due to the incorporation of the MAX Phase number of pores would not increase.

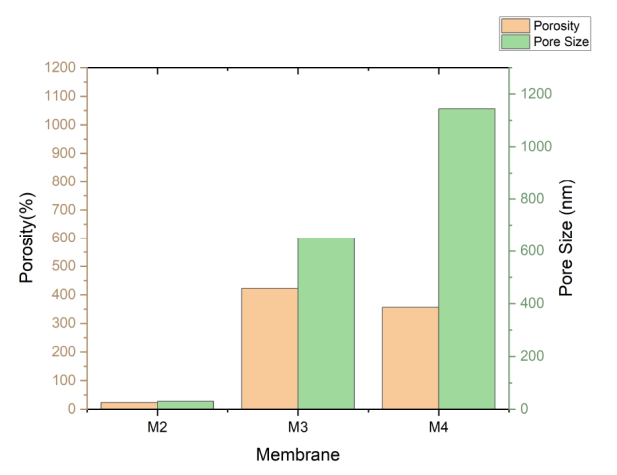


**Figure 2:** Variation of membrane porosity (%) and average pore size (nm) as a function of Mo<sub>2</sub>TiAlC<sub>2</sub> loading, illustrating the influence of MAX phase content on membrane morphology.

# 3.1.2. Membrane Chemical Composition and Molecular Structure

The chemical composition and molecular structure analysis were conducted using a Fourier Transform

Infrared Spectroscopy. The Figure **3** depicts the FTIR spectra before filtration of Bovine Serum Albumin. The peak observed was at 1402 cm<sup>-1</sup>, which corresponds to the stretching vibration of C-H [21]. The peak appeared at 1178 cm<sup>-1</sup> corresponds to the vibrational modes of C-F bonds [21]. These peaks are a sign of the presence of C-H and C-F functional groups, as would be expected in the PVDF polymer [21]. These two peaks showed no noticeable change with the incorporation of the MAX Phase, confirming that the structural integrity of the PVDF matrix remained unaffected.

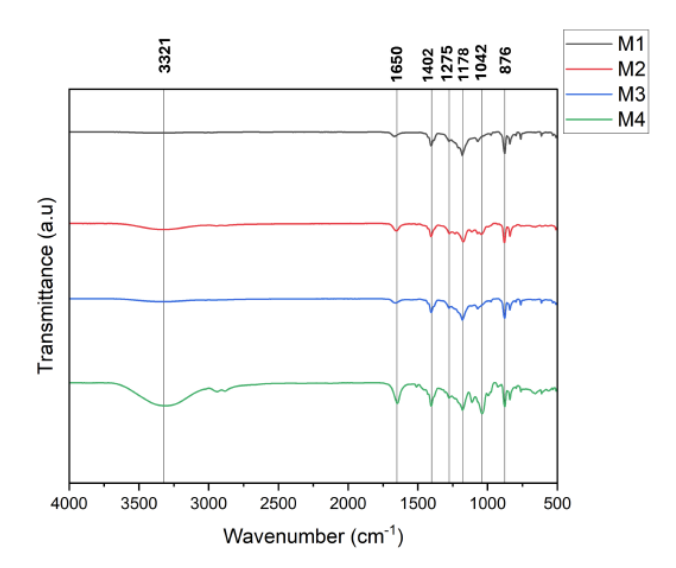


**Figure 3:** FTIR spectrum of the membranes before filtration, indicating the characteristic functional groups of PVDF and the presence of  $Mo_2TiAlC_2$ -related peaks.

The peak at 1650 cm<sup>-1</sup> depicts the -C=O bonds, and the peak at 1275 cm<sup>-1</sup> depicts the C-N bonds [17, 23]. The peaks are formed due to the successful deposition of PVP, and these bands are characteristic of the acylamino functional groups present in the PVP structure [23]. The hydrophilicity of the membranes was enhanced by the addition of PVP. This is because the hydrophilicity was derived from the interactions of polar attractive forces and hydrogen bonds between acylamino and water molecules [23]. The peaks at 876 and 1042 cm<sup>-1</sup> correspond to C-C and C-O stretching vibrational modes [24]. When the membranes before and after filtration were compared, a reduction in these two peaks was observed, indicating that the hydrophilic characteristics imparted by PVP were diminished after filtration.

The peak at 3321 cm<sup>-1</sup>, corresponds to N-H stretching vibration, indicating the presence of amine or amide functional groups prior to filtration [25]. This peak is formed before filtration and then vanishes after

filtration. This is due to Catalytic N-H Bond Activation and Breaking. Transition metal complexes, such as those present in the Mo<sub>2</sub>TiAlC<sub>2</sub> MAX phase, can weaken and activate N-H bonds by coordinating to them, making the bonds more reactive and easier to break, which can result in new bond formation and the loss of the original N-H bond [25].

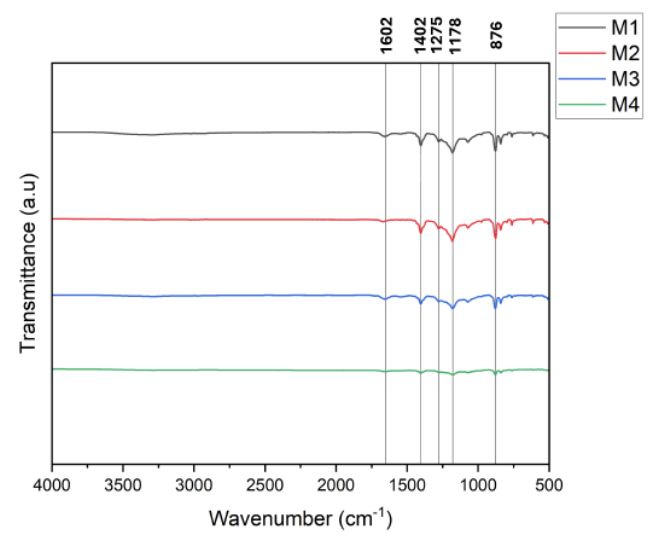


**Figure 4:** FTIR spectrum of the membranes after filtration, highlighting potential changes in functional groups and surface chemistry following protein filtration.

# 3.2. Membrane Performance

# 3.2.1. Bovine Serum Albumin (BSA) Rejection

A homemade dead-end filtration apparatus was used to determine the BSA rejection ratio. A 1000mg/L BSA concentration solution was used as the feed. The UV-Visible Spectroscopy was performed to find the

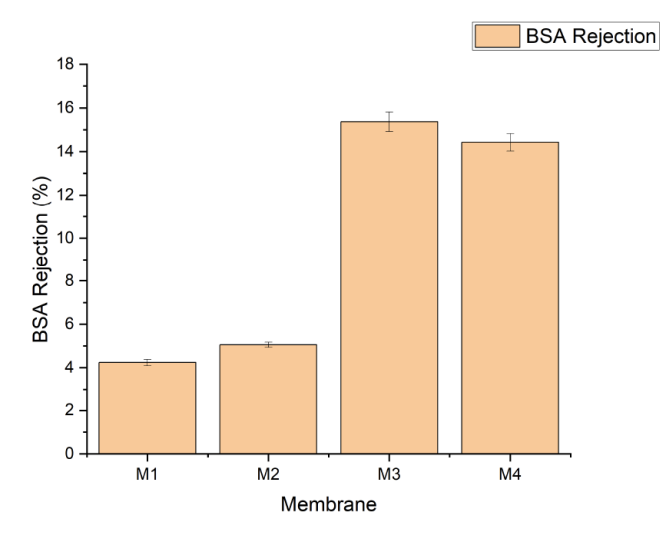


**Figure 5:** BSA rejection performance of neat PVDF and Mo<sub>2</sub>TiAlC<sub>2</sub>/PVDF composite membranes, demonstrating the effect of MAX phase addition on separation efficiency.

concentration of the solution before and after filtration. The M1 and M2 membranes have the lowest rejection, while M3 has the highest rejection. The reason for the better rejection of M3 and M4 can be seen from Figure 4. After filtration, the M1 and M2 membrane peaks decreased slightly, which resulted in lower BSA rejection. The peaks in M3 and M4 have almost vanished and have a drastic BSA rejection. However, the M3 membrane exhibited the highest protein rejection of 84.9%, which is slightly lower than the BSA rejection reported for the Ti<sub>3</sub>AlC<sub>2</sub> MAX phase/PVDF membrane (90.6%) [21].

# 4. CONCLUSION

This study utilised the composite MAX phase Mo<sub>2</sub>TiAlC<sub>2</sub> to synthesise PVDF membranes ultrafiltration applications. Different amounts Mo<sub>2</sub>TiAlC<sub>2</sub> were incorporated to determine the optimum nanoparticle-to-polymer ratio. Various techniques were employed to examine and monitor the structural and performance changes induced by the additive. The performance of the nanocomposite membranes was evaluated through BSA rejection tests. The incorporation of Mo<sub>2</sub>TiAlC<sub>2</sub> increased the pore diameters of the membranes approximately 30 nm, 650 nm, and 1144 nm, respectively. However, these effects were significant only up to a concentration of 0.6 wt%. Among all samples, the M3 membrane exhibited the highest BSA rejection of 84.9%. The findings of this study demonstrate the potential of Mo<sub>2</sub>TiAlC<sub>2</sub> as an effective additive for minimising PVDF membrane fouling, warranting further investigation into its long-term performance and applicability in complex feed systems. Future work will focus on conducting extended filtration experiments to assess membrane durability and antifouling behaviour over time, as well as exploring the performance of the Mo<sub>2</sub>TiAlC<sub>2</sub>/PVDF mixed matrix membranes in treating actual wastewater samples to validate their practical applicability under realistic operating conditions.

# **ACKNOWLEDGEMENTS**

The financial support provided by Dr. W. G. C. Kumarage for SEM analyses is gratefully acknowledged.

## **REFERENCES**

[1] Tijana Uroševic and Katarina Trivunac. Achievements in lowpressure membrane processes microfiltration (MF) and ultrafiltration (UF) for wastewater and water treatment. In Current Trends and Future Developments on (Bio-) Membranes. Elsevier 2020; pp. 67-107.

https://doi.org/10.1016/B978-0-12-817378-7.00003-3

- [2] Inamuddin RB, Asiri AM. Self-Standing Substrates: Materials and Applications. Engineering Materials. Springer International Publishing, Cham 2020. https://doi.org/10.1007/978-3-030-29522-6
- [3] Aryanti PTP, Hakim AN, Widodo S, Widiasa IN, Wenten IG. Prospect and Challenges of Tight Ultrafiltration Membrane in Drinking Water Treatment. IOP Conference Series: Materials Science and Engineering 2018; 395: 012012. https://doi.org/10.1088/1757-899X/395/1/012012
- [4] Futselaar H, Schonewille H, van Dalfsen H. Ultrafiltration technology for potable, process and waste water treatment. Membrane Science and Technology/Membrane Science and Technology Series 2003.
- [5] Universiti Pendidikan Sultan Idris, R. Mohamat, A. B. Suriani, Universiti Pendidikan Sultan Idris, A. Mohamed, Universiti Pendidikan Sultan Idris, Muqoyyanah, Universiti Pendidikan Sultan Idris, M. H. D. Othman, Universiti Teknologi Malaysia, R. Rohani, Universiti Kebangsaan Malaysia, M. H. Mamat, Universiti Teknologi MARA (UiTM), M. K. Ahmad, Universiti Tun Hussein Onn Malaysia, M. F. Malek, Universiti Teknologi MARA (UiTM), H. P. S. Abdul Khalil, Universiti Sains Malaysia, K. Ali, and University of Agriculture Faisalabad. Recent Advances for Wastewater Treatment on Polyvinylidene Fluoride-Based Membrane: A Review. International Journal of Integrated Engineering 2024; 16(5). https://doi.org/10.30880/iiie.2024.16.05.039
- [6] Zou D, Lee YM. Design strategy of poly(vinylidene fluoride) membranes for water treatment. Progress in Polymer Science 2022. <a href="https://doi.org/10.1016/j.progpolymsci.2022.101535">https://doi.org/10.1016/j.progpolymsci.2022.101535</a>
- [7] Herlambang Abriyanto. Hydrophilic Modification of PVDF Membrane: A Review.
- [8] Improving the hydrophilicity and antifouling performance of PVDF membranes via PEI amination and further poly (methyl vinyl ether-alt-maleic anhydride) modification. Reactive and Functional Polymers 2023; 189: 105610. https://doi.org/10.1016/j.reactfunctpolym.2023.105610
- [9] Khulbe KC, Matsuura T. Membrane Modification. Springer International Publishing 2021; 135-170. <a href="https://doi.org/10.1007/978-3-030-64183-2\_4">https://doi.org/10.1007/978-3-030-64183-2\_4</a>
- [10] Van Der Bruggen B. Chemical modification of polyethersulfone nanofiltration membranes: A review. Journal of Applied Polymer Science 2009; 114(1): 630-642. <a href="https://doi.org/10.1002/app.30578">https://doi.org/10.1002/app.30578</a>
- [11] Saffarimiandoab F, Gul BY, Tasdemir RS, Ilter SE, Unal S, Tunaboylu B, Menceloglu YZ, Koyuncu I. A review on membrane fouling: Membrane modification. Desalination and Water Treatment 2021; 216: 47-70. https://doi.org/10.5004/dwt.2021.26815
- [12] Miller DJ, Dreyer DR, Bielawski CW, Paul DR, Freeman BD. Surface Modification of Water Purification Membranes. Angewandte Chemie International Edition 2017; 56(17): 4662-4711. https://doi.org/10.1002/anie.201601509
- [13] Zhou A, Liu Y, Li S, Wang X, Ying G, Xia Q, Zhang P. From structural ceramics to 2D materials with multi-applications: A review on the development from MAX phases to MXenes. Journal of Advanced Ceramics 2021; 10(6): 1194-1242. https://doi.org/10.1007/s40145-021-0535-5
- [14] Bakardjieva S, Klie R. The Morphology of TiiAlC (M2AX) and TiiC (MXene) Sheets Revealed by HAADF STEM Analysis. Microscopy and Microanalysis 2018; 24(S1): 156-157. https://doi.org/10.1017/S1431927618001277

- [15] Luxa J, Kupka P, Fedor Lipilin, Jiři S, Subramani A, Lazar P, Sofer Z. Hydrogen Evolution Reaction Activity in Mo<sub>2</sub>TiC<sub>2</sub> Tx MXene Derived from Mo<sub>2</sub> TiAlC<sub>2</sub> MAX Phase: Insights from Compositional Transformations. ACS Catalysis 2024; 14(20): 15336-15347. https://doi.org/10.1021/acscatal.4c04099
- [16] Ali MS, Rayhan MA, Ali MA, Parvin R, Islam AKMA. New MAX Phase Compound Mo<sub>2</sub>TiAlC<sub>2</sub>: First-principles Study. Journal of Scientific Research 2016; 8(2): 109-117. https://doi.org/10.3329/jsr.v8i2.25057
- [17] Zhang J, Xu Z, Mai W, Min C, Zhou B, Shan M, Li Y, Yang C, Wang Z, Qian X. Improved hydrophilicity, permeability, antifouling and mechanical performance of PVDF composite ultrafiltration membranes tailored by oxidized low-dimensional carbon nanomaterials. Journal of Materials Chemistry A 2013; 1(9): 3101. https://doi.org/10.1039/c2ta01415q
- [18] Ayyaru S, Dinh TTL, Ahn Y-H. Enhanced antifouling performance of PVDF ultrafiltration membrane by blending zinc oxide with support of graphene oxide nanoparticle. Chemosphere 2020; 241: 125068. https://doi.org/10.1016/j.chemosphere.2019.125068
- [19] Ma C, Hu J, Sun W, Ma Z, Yang W, Wang L, Ran Z, Zhao B, Zhang Z, Zhang H. Graphene oxide-polyethylene glycol incorporated PVDF nanocomposite ultrafiltration membrane with enhanced hydrophilicity, permeability, and antifouling performance. Chemosphere 2020; 253: 126649. https://doi.org/10.1016/j.chemosphere.2020.126649
- [20] Ostovar A, Tarkhani M, Mousavi SA, Asadollahi M. Surface modification of GO/PVDF composite membrane by MXene/protonated g-C<sub>3</sub>N<sub>4</sub> nanosheets hybrids with improved dye separation and antifouling properties. Polymer Engineering & Science 2024. https://doi.org/10.1002/pen.26566
- [21] Abood TW, Shabeeb KM, Alzubaydi AB, Sh. Majdi H, Al-Juboori RA, Alsalhy QF. Effect of MAX Phase Ti<sub>3</sub>ALC<sub>2</sub> on the Ultrafiltration Membrane Properties and Performance. Membranes 2023; 13(5): 456. https://doi.org/10.3390/membranes13050456
- [22] Abood T, Shabeeb K, Alzubaydi A, Goh P, Ismail A, Zrelli A, Alsalhy Q. Effect of MXene Ti<sub>3</sub>C<sub>2</sub> on the PVDF ultrafiltration membrane properties and performance. Engineering and Technology Journal 2024; 0(0): 1-14. https://doi.org/10.30684/eti.2024.145778.1663
- [23] Hou L, Zhang J, Zhang X, Wu Z, Wang Q. Enhancement of PVDF membrane anti-fouling ability based on critical flux: Effects of fabrication parameters and membrane properties. Desalination and Water Treatment 2025; 321: 101061. https://doi.org/10.1016/j.dwt.2025.101061
- [24] Zhang W, Fu C, Low J, Duan D, Ma J, Jiang W, Chen Y, Liu H, Qi Z, Long R, Yao Y, Li X, Zhang H, Liu Z, Yang J, Zou Z, Xiong Y. High-performance photocatalytic nonoxidative conversion of methane to ethane and hydrogen by heteroatoms-engineered TiO<sub>2</sub>. Nature Communications 2022; 13(1): 2806. https://doi.org/10.1038/s41467-022-30532-z
- [25] Khivantsev K, Biancardi A, Fathizadeh M, Almalki F, Grant JL, Tien HN, Shakouri A, Blom DA, Makris TM, Regalbuto JR, Caricato M, Yu M. Catalytic N-H Bond Activation and Breaking by a Well-Defined Coll<sub>1</sub>O<sub>4</sub> Site of a Heterogeneous Catalyst. ChemCatChem 2018; 10(4): 736-742. https://doi.org/10.1002/cctc.201701268

Received on 11-08-2025 Accepted on 16-09-2025 Published on 21-10-2025

https://doi.org/10.6000/1929-5995.2025.14.17

# © 2025 Bandara and Samaranayaka.

This is an open-access article licensed under the terms of the Creative Commons Attribution License (<a href="http://creativecommons.org/licenses/by/4.0/">http://creativecommons.org/licenses/by/4.0/</a>), which permits unrestricted use, distribution, and reproduction in any medium, provided the work is properly cited.